Neuron, Vol. 24, 401–414, October, 1999, Copyright ©1999 by Cell Press

Essential Role for TrkB Receptors in Hippocampus-Mediated Learning

Liliana Minichiello,[1] Martin Korte,[2] David Wolfer,[3] Ralf Kühn,[4,9] Klaus Unsicker,[5] Vincenzo Cestari,[6] Clelia Rossi-Arnaud,[7] Hans-Peter Lipp,[3] Tobias Bonhoeffer,[2] and Rüdiger Klein[1,8]

[1]European Molecular Biology Laboratory
Meyerhofstrasse 1
69117 Heidelberg
Germany

[2]Max-Planck Institute of Neurobiology
Am Klopferspitz 18a
D-82152 Martinsried
Germany

[3]Anatomisches Institut
Universität Zürich
Winterthurerstrasse 190
CH-8057 Zürich
Switzerland

[4]Institute for Genetics
University of Cologne
Weyertalstrasse 121
D-50931 Cologne
Germany

[5]Department of Anatomy and Cell Biology III
University of Heidelberg
Im Neuenheimer Feld 307
D-69120 Heidelberg
Germany

[6]Istituto di Psicobiologia e Psicofarmacologia (CNR)
Viale Marx 15
00137 Roma
Italy

[7]Dipartimento di Psicologia
Universitá di Roma "La Sapienza"
Piazzale Aldo Moro 5
00185 Roma
Italy

Summary

Brain-derived neurotrophic factor (BDNF) and its receptor TrkB regulate both short-term synaptic functions and long-term potentiation (LTP) of brain synapses, raising the possibility that BDNF/TrkB may be involved in cognitive functions. We have generated conditionally gene targeted mice in which the knockout of the *trkB* gene is restricted to the forebrain and occurs only during postnatal development. Adult mutant mice show increasingly impaired learning behavior or inappropriate coping responses when facing complex and/or stressful learning paradigms but succeed in simple passive avoidance learning. Homozygous mutants show impaired LTP at CA1 hippocampal synapses. Interestingly, heterozygotes show a partial but substantial reduction of LTP but appear behaviorally normal. Thus, CA1 LTP may need to be reduced below a certain threshold before behavioral defects become apparent.

[8]To whom correspondence should be addressed (e-mail: klein@embl-heidelberg.de).
[9]Present address: Artemis Pharmaceuticals GmbH, Neurather Ring 1, D-51063 Köln, Germany.

Introduction

Brain-derived neurotrophic factor (BDNF) belongs to a small family of secreted proteins collectively known as the neurotrophins, including nerve growth factor (NGF), neurotrophin-3 (NT-3), and neurotrophin-4 (NT-4) (Henderson, 1996). Most functions of neurotrophins are mediated by the Trk family of tyrosine kinase receptors (Barbacid, 1995). The interaction of neurotrophins with Trk receptors is specific: NGF binds TrkA, BDNF and NT-4 both bind TrkB, and NT-3 binds with the highest affinity to TrkC but is also capable of signaling through TrkA and TrkB (Davies et al., 1995; Huang et al., 1999). The spectrum of biological activities of neurotrophins is quite diverse. In the peripheral nervous system (PNS), neurotrophins are essential for the survival of most sensory and sympathetic neurons before and during target innervation (Henderson, 1996; Lewin and Barde, 1996; Davies, 1997; Fritzsch et al., 1997). In the central nervous system (CNS), a survival function of neurotrophins is less obvious. Mild yet significant increases of TUNEL positive cells were found in hippocampus and neocortex of *trkB* null mice (Alcantara et al., 1997), and cell death was greatly enhanced in *trkB*/*trkC* double mutants, suggesting that TrkB and TrkC receptors cooperate in promoting the survival of specific CNS neuron populations (Minichiello and Klein, 1996). However, due to the premature death of *trkB* and *trkC* mutant mice, it remained unclear whether or not this defect would result in a decrease in cell numbers in the adult.

In the intact CNS, neurotrophins promote structural changes in axonal and dendritic arbors. For example, BDNF and NT3 have opposing roles in regulating the growth of basal dendrites of pyramidal neurons of the developing neocortex, suggesting interesting differences in the signaling capabilities of the highly related TrkB and TrkC receptors (Shieh and Ghosh, 1997; McAllister et al., 1999). Neurotrophins regulate the activity-driven rearrangements that form eye-specific layers in the lateral geniculate nucleus and in ocular dominance columns in the visual cortex (Katz and Shatz, 1996; Penn et al., 1999). Besides promoting structural changes, neurotrophins appear to modulate both short-term and long-term synaptic transmission (McAllister et al., 1999). For example, lack of BDNF in *BDNF* null mutant mice impaired CA3–CA1 hippocampal long-term potentiation (Korte et al., 1995; Patterson et al., 1996; Pozzo-Miller et al., 1999). This impairment could be rescued by supplying exogenous BDNF in vitro (Patterson et al., 1996) or by virus-mediated gene transfer (Korte et al., 1996), suggesting that the defect is a consequence of lack of an acute function of BDNF rather than reflecting a developmental function of BDNF.

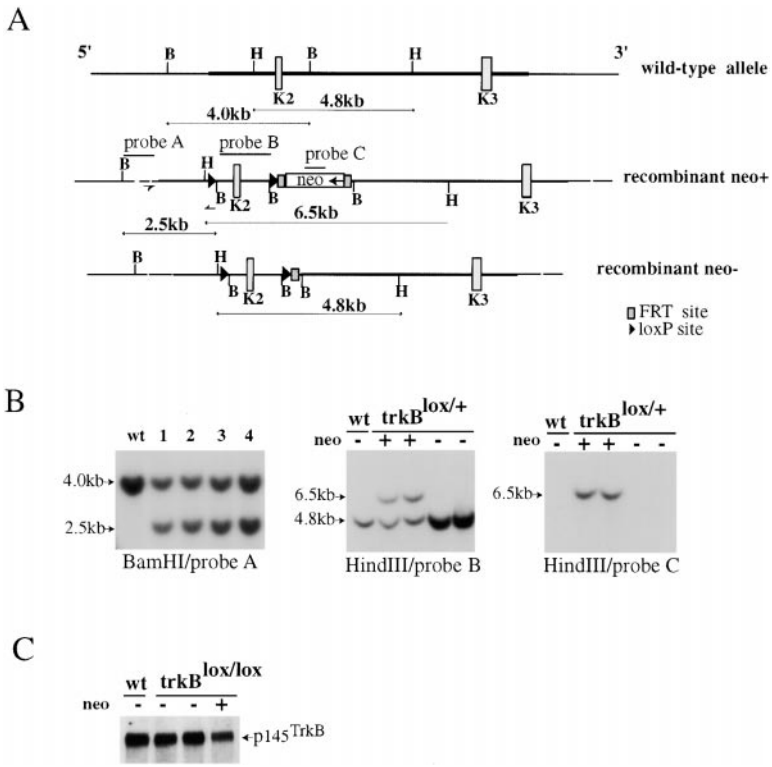

Figure 1. Generation of the Floxed *trkB* Gene

(A) Schematic representation of the second (K2) and third (K3) exons of the tyrosine kinase region of the mouse *trkB* locus in wild-type, recombinant (*neo*$^+$), and recombinant (*neo*$^-$) alleles. The *neo* gene was removed in vivo by crossing *trkB*$^{lox/+}$ (*neo*$^+$) mice with transgenic mice expressing the Flp recombinase under control of the human β-actin promoter (Dymecki, 1996; Minichiello et al., 1998).

(B) Southern blot analyses of targeted ES cell clones (probe A, left panel), of *trkB*$^{lox/+}$ *neo*$^+$ and *neo*$^-$ mice using either a probe encompassing exon K2 (probe B, middle panel) or a *neo* probe (probe C, right panel). Note that the HindIII fragments detected by probe B in wild-type and *trkB*$^{lox/+}$ *neo*$^-$ mice only differ by the insertion of the loxP/FRT sites and cannot be resolved in the gel.

(C) Western blot analysis of gp145^{TrkB} protein in brains of *trkB*$^{lox/lox}$ mice. Protein lysates were prepared from adult brains of wild-type (wt) and *trkB*$^{lox/lox}$ mice, either in the absence (−) or presence (+) of the *neo* cassette, subjected to immunoprecipitation (IP) using a pan-Trk antiserum followed by Western blot analysis using a specific anti-TrkB antiserum. Note the reduction of gp145^{TrkB} levels in the presence of the *neo* cassette. All further work was therefore done with *trkB*$^{lox/lox}$ (*neo*$^-$) mice.

A major limitation for the study of neurotrophin functions in the CNS has been the fact that the majority of mice deficient in either BDNF or TrkB die sometime between birth and weaning age, most likely due to respiratory failure (Erickson et al., 1996). Thus, it has been unclear whether the impairments in synaptic functions would result in behavioral defects and if so, whether such defects would be limited to complex learning behavior or affect basic functions such as locomotion or vision. Because of the lack of proper animal models, behavioral tests had so far been limited to heterozygous *BDNF* mutants, with controversial results (Linnarsson et al., 1997; Montkowski and Holsboer, 1997). Our own tests on heterozygous *trkB*/*trkC* double mutants had not revealed general neurological impairments, nor defects in spatial learning abilities (D. W. et al., unpublished data). Moreover, behavioral tests using null mutant mice only allow limited conclusions, because components other than the target may have been indirectly damaged, and the phenotype may be a complex syndrome due to direct effects of the mutation and subsequent compensations by the neural system.

To circumvent these problems, we used the phage P1-derived CRE/loxP recombination system to restrict the *trkB* gene knockout with respect to space and time, i.e., to postmitotic neurons of the anterior forebrain. These conditional *trkB* knockout mice were viable and developed without gross morphological defects. We now show that adult mutant mice exhibit a severe impairment in spatial learning tasks and show reduced hippocampal LTP compared to wild-type mice. Since recombination did not start until the end of the second postnatal week, at a time when many of the CNS neuronal pathways are established, these results suggest that the BDNF/TrkB system directly regulates complex behavior.

Results

Region-Specific and Postnatal Inactivation of the Catalytic Isoform of *trkB*

We flanked (floxed) the second exon of the *trkB* tyrosine kinase region with two loxP sites by homologous recombination in ES cells (Figure 1A) and derived germline targeted offspring carrying one floxed allele (*trkB*$^{lox/+}$ mice). Excision of this exon by the CRE recombinase would eliminate catalytically active gp145^{TrkB} receptors without interfering with the expression of truncated TrkB isoforms (Klein et al., 1993), whose functions are ill defined. The *neo* selection marker was flanked by FRT sites and was excised in vivo by crossing with transgenic mice expressing the Flp recombinase (Figure 1B) (Dymecki, 1996; Minichiello et al., 1998). While the expression of gp145^{TrkB} receptors was reduced in *neo*$^+$ mice, expression increased to normal levels after excision of the *neo* cassette (Figure 1C). All subsequent work was performed using *neo*$^-$ mice.

We next generated transgenic mice expressing the CRE recombinase under control of the CaMKIIα promoter (Figure 2A; see Experimental Procedures) (Mayford et al., 1996). To assess the regional and temporal pattern of CRE activity in vivo, transgenic line CaMKII–CRE-159 (CRE-159) was crossed to a lacZ transgenic reporter mouse (Akagi et al., 1997), and brain sections were analyzed for CRE recombination by X-Gal staining (Figures 2B–2F). Before postnatal day 15 (P15), no or little X-Gal staining was detected in doubly transgenic

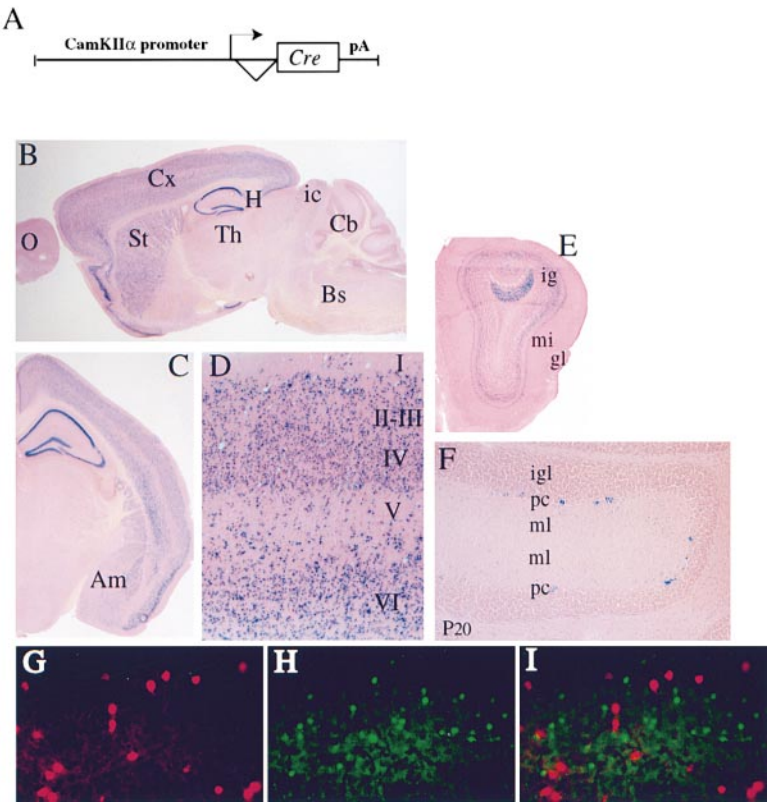

Figure 2. Recombination Pattern of the CaMKII–CRE (159) Transgenic Line

(A) Schematic representation of the CaMKII–CRE transgene. Triangle represents intron sequences. pA, polyadenylation signal. (B–F), Spatial pattern of CRE activity. Postnatal day 60 brains (except [F]) of doubly transgenic lox-lacZ;CRE-159 mice were stained for β-galactosidase activity using X-gal and counter stained by eosin. (B) Parasagittal section (anterior left) with positive signals in neocortex (Cx), striatum (St), and hippocampus (H). Little or no staining in other brain areas, including olfactory bulb (O), thalamus (Th), inferior colliculus (ic), cerebellum (Cb), and brain stem (Bs). (C) Coronal section showing positive staining in neocortex (including posterior limbic, motor, somatosensory, and piriform cortex), amygdala (Am), and hippocampus. (D) High-power photograph of somatosensory cortex showing strong recombination in layers II–IV and VI. (E) Coronal section of olfactory bulb showing some staining in the internal granular layer. (F) Sagittal section of the cerebellum of a P20 mouse brain with few labeled Purkinje neurons. (G–I) Immunofluorescence showing parvalbumin (G), CRE protein (H), and the overlay of the two signals (I) in somatosensory cortex of P90 CaMKII–CRE mice. Note the absence of CRE protein in parvalbumin-positive interneurons. Abbreviations: igl, internal granular layer; ml, molecular layer; pc, purkinje cell layer; ig, internal granular layer of olfactory bulb; mi, mitral layer of olfactory bulb; gl, glomerular layer olfactory bulb. Magnifications: (B), 1.1×; (C), 1.5×; (D) and (E), 100×; (F), 50×; and (G)–(I), 200×.

mice (data not shown). At or after P20, CRE recombination was specifically observed in the forebrain in a pattern somewhat resembling the previously published strain T29-2 (Tsien et al., 1996), including pyramidal neurons of the hippocampus (strong staining in CA1, lighter staining in CA3 and dentate gyrus), neocortex, striatum, and amygdala. Few labeled cells were observed in the cerebellum (Purkinje cells) and olfactory bulbs (Figures 2E and 2F) and inferior colliculus (data not shown). This pattern of recombination matches very well the expression of functional TrkB receptors in the adult, which includes cerebral cortex, hippocampus, striatum, and amygdala (Fryer et al., 1996). TrkB is expressed in both excitatory pyramidal and inhibitory interneurons, which express the Ca^{2+}-binding proteins parvalbumin and calbindin (Gorba and Wahle, 1999). Double immunofluorescence for CRE protein and parvalbumin revealed no overlapping expression indicating that CRE expression is absent in inhibitory interneurons (Figures 2G–2I). Similar lack of CRE recombination in interneurons of the CA1 region was observed with an independently generated CaMKII–CRE mouse line by costaining for CRE recombination (β-galactosidase) and both parvalbumin and calbindin (B. Xu and L. Reichardt, personal communication).

To inactivate TrkB in the postnatal forebrain, we crossed heterozygous *trkB* null mice (Klein et al., 1993) bearing the CaMKII–CRE transgene to homozygous $trkB^{lox/lox}$ mice, to generate $trkB^{lox/null}$;CaMKII–CRE mice (or simply "*trkB*–CRE" mice). Conditional mutants were viable and fertile and showed no gross pathologies (see below). Western analysis of $gp145^{TrkB}$ protein revealed a consistent 2-fold reduction in adult heterozygotes ($trkB^{lox/+}$;CaMKII–CRE or $trkB^{lox/null}$ mice) and a nearly complete loss of the protein (on average 86%) in hippocampus and anterior forebrain in all *trkB*–CRE mice tested ($n = 8$) (Figure 3A). As expected from the lacZ reporter analysis, no CRE-mediated loss of $gp145^{TrkB}$ protein was observed in adult spinal cord (data not shown), cerebellum and brain stem, and in early postnatal stages (Figure 3A). A time course of TrkB protein removal in hippocampus revealed that at P20 a reduction in TrkB protein was first detectable and that at P39 the loss of TrkB protein was similar to P90 (Figures 3A and 3B). Besides hippocampus and neocortex, striatum and amygdala play important roles in learning processes (see below). We microdissected these brain areas from individual adult mice and determined TrkB protein levels by Western blot analysis. As shown in Figure 3C, removal of TrkB protein occurred with high efficiency in striatum and amygdala.

Normal Brain Morphology of *trkB*–CRE Mice

In early postnatal CNS, TrkB receptor signaling is implicated in neuronal survival and differentiation (Minichiello and Klein, 1996; Alcantara et al., 1997). In 6- to 15-week-old *trkB*–CRE mice, however, we did not find any signs of increased cell death, neither by detecting pyknotic nuclei in Nissl stained sections nor by TUNEL staining

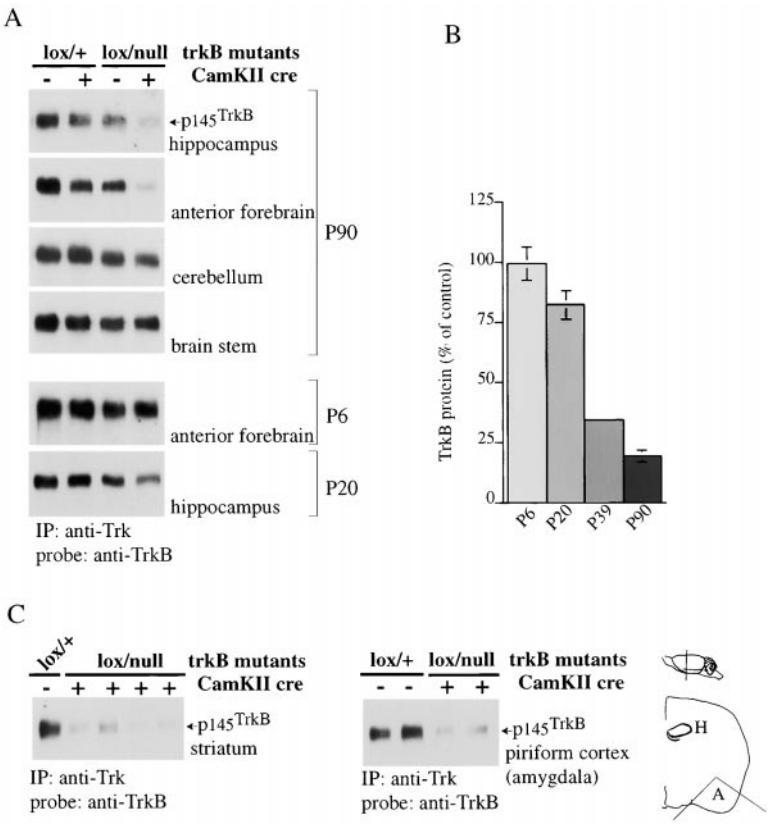

Figure 3. Spatial Pattern and Time Course of gp145^{TrkB} Protein Removal from *trkB*–CRE Mice

(A) Protein lysates were prepared from the indicated tissues of postnatal day 90 (P90), P6, and P20 *trkB*$^{lox/+}$ and *trkB*$^{lox/null}$ mice, either in the absence (−) or presence (+) of the CaMKII–CRE transgene, subjected to IP and Western blot analysis (probe) as described in the legend of Figure 1. Note the approximately 2-fold reduction in gp145^{TrkB} in *trkB*$^{lx/null}$ compared to *trkB*$^{lx/+}$ mice due to the presence of the *trkB*^{null} allele. No effects of the CRE transgene are seen in cerebellum, brain stem, and early postnatal forebrain. The residual signals observed in *trkB*–CRE hippocampus and forebrain were confirmed to be gp145^{TrkB} protein and not cross-reactivity with the related TrkC receptor by using a TrkB-specific monoclonal antibody (Klein et al., 1993) (data not shown).

(B) Time course of TrkB diminution in the hippocampus of *trkB*–CRE mice. TrkB protein levels were quantified by measuring the intensity of the Western blot signal with the NIH-Image system. Levels are expressed as percentage of control mice (*trkB*$^{lx/null}$ in the absence of CRE) (n = 2–8 for each time point).

(C) TrkB protein expression in individual *trkB*–CRE mice in microdissected striatum (n = 4) and amygdala (n = 2). In the case of the amygdala, a coronally sectioned region of 300 μm was prepared and the piriform cortex punched out as indicated in the schematic drawing for subsequent Western analysis. The amygdala represents a major portion of this section.

(data not shown). The neocortex showed the normal layered structure, and cortical neurons had normal appearance based on calretinin, parvalbumin, and neurofilament staining (data not shown). Merely in 3-month-old mutants, the thickness of the visual cortex appeared mildly (approximately 10%) reduced (data not shown). CA1 through CA3 regions and dentate gyrus of the hippocampus appeared normal based on Nissl staining pattern and neurofilament immunoreactivity, indicating that the mutation did not affect hippocampal architecture and cell/neurite density (Figures 4A–4D). Calbindin immunostaining (Minichiello and Klein, 1996) revealed normal mossy fiber projections to the CA3 region (Figures 4E and 4F). In the CA1 region of *trkB*–CRE mice, the intensity and pattern of the dendritic marker MAP2 was indistinguishable from controls (Figures 4G and 4H). Golgi stains of CA1 pyramidal neurons revealed qualitatively normal cell morphology with respect to soma size, cell shape, and dendritic branching (Figures 4I and 4J). Using electron microscopy, *trkB*–CRE mice showed normal structural features of pyramidal neurons and astroglia. In contrast to the findings in *trkB*$^{-/-}$ mice (Martinez et al., 1998), there was a normal asymmetric synapse morphology, including synaptic vesicles and postsynaptic density (Figures 4K and 4L). Preliminary counts did not suggest reductions in synapse number (data not shown). *BDNF*$^{-/-}$ mice had previously been found to have defects in CNS myelination (Cellerino et al., 1997). We found that the number of myelinated axons in the CA1 region of the hippocampus was reduced by 23% in *trkB*–CRE mice compared to *trkB*$^{lox/+}$ mice (Table 1). Heterozygotes were not affected, and this deficit did not result in reduced synaptic responses to electrical stimulation (see below). Taken together, these results indicate that postnatal reduction of TrkB from the forebrain did not cause gross morphological alterations.

trkB–CRE Mice Do Not Learn the Morris Water Maze

The normal lifespan and the lack of significant developmental abnormalities of *trkB*–CRE mice allowed us to perform behavioral tests to assess the importance of TrkB receptor signaling for complex cognitive functions as well as their physiological correlates. Spontaneous activity of *trkB*–CRE mice in an open field arena was similar to controls, and *trkB*–CRE mice were not excessively hyperactive, such as mice with defects in the dopaminergic system (Xu et al., 1994). In fact, dopamine levels in the striatum of *trkB*–CRE mice, assessed by HPLC and amperometric detection, were normal (data not shown). Furthermore, we did not find evidence for loss of dopaminergic neurons in *trkB*–CRE mice, based on the normal immunoreactivity for tyrosine hydroxylase in striatum and substantia nigra (data not shown).

To assess spatial learning, mice were tested in the Morris water maze (Morris, 1982), in which mice have to swim in opaque water and learn, using external visual

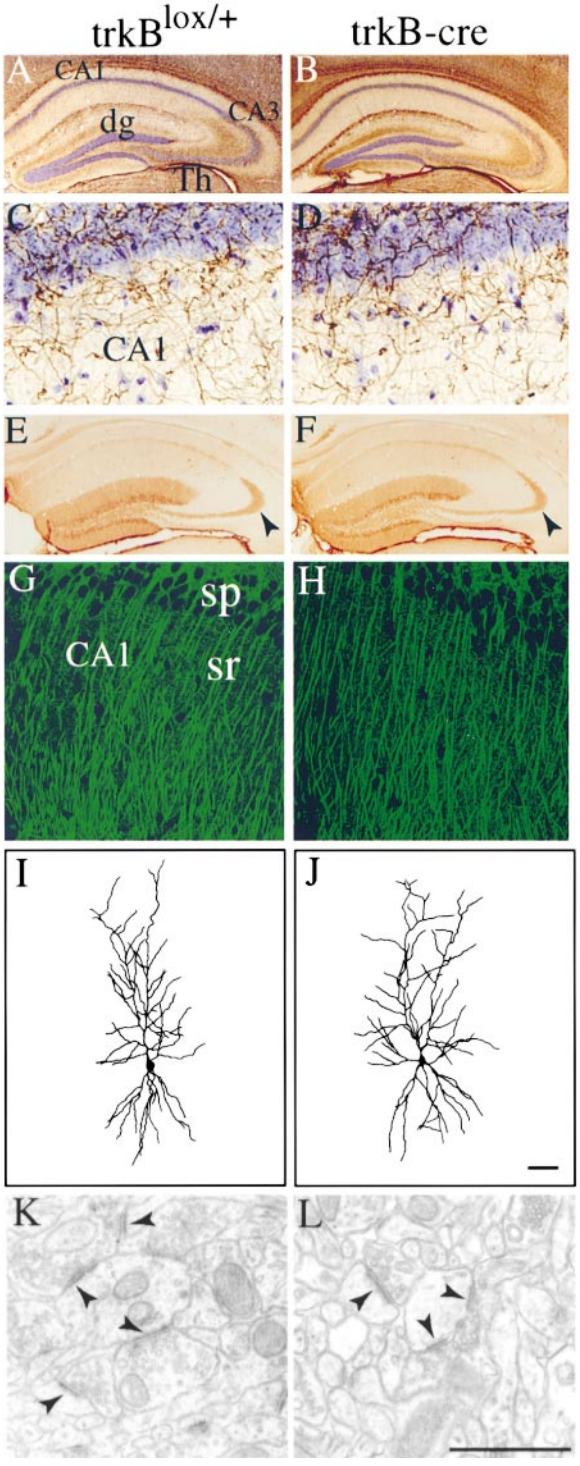

Figure 4. Anatomy of the Hippocampus of Adult Mice

(A), (C), (E), (G), (I), and (K), *trkB*$^{lox/+}$ control; (B), (D), (F), (H), (J), and (L), *trkB*–CRE mice. (A–D) Nissl (blue) and antineurofilament (brown) double staining and (E and F) calbindin immunostaining of hippocampus. Mossy fibers are indicated with arrowhead; (G and H) MAP2 immunofluorescence in CA1 region showing the pyramidal cell layer (SP) and stratum radiatum (SR); (I and J) Golgi-stained CA1 pyramidal neurons. No abnormalities observed with respect to soma size, cell shape, and dendritic branches; (K and L) ultrastructure of CA1 stratum radiatum showing normal asymmetric morphology of synapses in both wild-type controls and *trkB*–CRE mice. Magnifications: (A), (B), (E), and (F), 50×; (C) and (D), 630×; (G) and (H), 400×. Scale bar: (J), 50 μm; (L), 1 μm.

cues, to find a platform hidden beneath the water surface in a constant location. With the experimenter blind with respect to genotype, mice were trained for 30 trials in the hidden platform version (18 trials acquisition phase followed by 12 trials reversal with the platform in a new location). Afterward, a subgroup of animals was tested for 12 trials with the platform marked with a flag (visible test) and moved to a new location for every trial. In order to check the effects of prolonged training, the other subgroup received an additional 18 training trials in the hidden platform version (Figure 5A). To assess if the animals had remembered the location of the platform or whether they used nonspatial strategies to find the platform, each acquisition phase was followed by a probe trial, in which the platform was moved to the opposite quadrant. As in the open field test, the performance of wild-type, heterozygotes, and CRE-159 mice was statistically indistinguishable. In contrast, *trkB*–CRE mice were dramatically impaired in all phases of water maze training, except for the first trial where they showed swim times indistinguishable from controls (Figures 5A–5C). During both training phases with a hidden platform and despite extended training, *trkB*–CRE mice had to be qualified as complete nonlearners because their escape latencies (time required to reach the platform) did not decrease over time (Figure 5A). Their escape latencies began to decrease only when the platform was made visible, confirming that *trkB*–CRE mice are able to process visual information. Overall performance in the visible test remained poor compared to controls, an effect previously observed in hippocampal lesioned mice (Logue et al., 1997). The failure of *trkB*–CRE mice to learn the water maze test was largely due to their excessive wall hugging (thigmotaxis) and floating behavior (Figure 5B). Passivity was less prominent during the retest phase, indicating that it was not due to physical weakness. During probe trials, control mice crossed the former goal annulus more frequently than respective control sites in other quadrants (data not shown) and spent more time in a circular zone around the former goal (Figure 5C). In contrast, *trkB*–CRE mice showed no spatial preference for the goal area, neither in the first probe trial (ANOVA zone time: genotype $F(63,1) = 12.044$ $p < .0009$, interaction genotype*place not significant) nor after additional training in the second probe trial (ANOVA zone time: $F(21,1) = 19.072$ $p < .0003$, interaction genotype*place $F(21,1) = 9.861$ $p < .0049$).

Partial Impairment of *trkB*–CRE Mice in the Eight-Arm Radial Maze

These findings suggested that *trkB*–CRE mice had a severe defect in complex spatial learning requiring the establishment of long-term spatial reference memory, which includes both the memory of distant cues and learning how to use them. This process is classically impaired after hippocampal lesions (Morris, 1982). To test whether the failure in the water maze might have

Table 1. Reduction in the Number of Myelinated Axons in the CA1 Region of *trkB*–CRE Mice

Genotype	Number of Animals	Myelinated Axons/mm^2 ± SEM	Percentage Compared with *trkB*$^{lox/+}$
trkB$^{lox/+}$	3	2761 ± 154	
Heterozygotes	4	2908 ± 192	105
trkB–CRE	3	2114 ± 136	77[a]

Counts were taken from two different plains 50 μm apart from each animal (see the Experimental Procedures). Heterozygotes (*trkB*$^{lox/+}$; CaMKII–CRE or *trkB*$^{lox/null}$ mice) gave similar numbers and were pooled into one group. Statistical analysis carried out using Student's t-test.
[a] $P < 0.01$.

been caused by inappropriate behavioral coping with stressful situations, the mice were subjected to a less stressful task also known to depend on an intact hippocampus, the eight-arm radial maze (Olton et al., 1978; Rossi-Arnaud and Ammassari-Teule, 1998). During this test, mice run freely about the maze and are permitted to use olfactory, kinesthetic (consecutive choices to adjacent arms), and spatial information to perform the task. All eight arms were baited at the beginning of each session, and the baits were not replaced. Reentering a previously visited arm was counted as an error. This paradigm assesses the capacity of short-term spatial memory (working memory) by measuring whether the animals can remember a sequence of previously visited feeding sites. Analysis of the number of correct arm choices (during the first eight choices) in each trial showed that all mice learned the radial maze ($p = 0.0001$). Although the increase in correct responses was also significant in the mutants ($p = 0.005$), they showed significantly poorer learning compared to both wild-type and heterozygotes ($p < 0.0004$ and $p < 0.002$, respectively) (Figure 6A). The analysis of the error scores revealed significantly higher error scores in the mutants compared to wild-type and heterozygotes ($p < 0.0001$ and $p < 0.0003$, respectively) (Figure 6B). This indicates that the mutants committed more errors during their attempts to find the one or two last arms still containing baits, while control mice were merely correcting single errors committed during the last phase of the session, which is most demanding in terms of short-term spatial memory.

trkB–CRE Mice Succeed in Less Demanding Learning Tests

The complete failure in the more stressful water maze test compared to only partial failure in the eight-arm maze suggested abnormal coping responses to stress in *trkB*–CRE mice. We therefore analyzed their performance in simple learning tests involving aversive stimuli. The passive avoidance (one trial inhibitory avoidance) test makes use of the natural tendency of mice to move from an illuminated into a dark compartment (Cahill and McGaugh, 1990). During training, the mouse is placed into the illuminated compartment, and the time to enter the dark compartment is recorded (step-through latency). Mice then receive two electric foot shocks in the

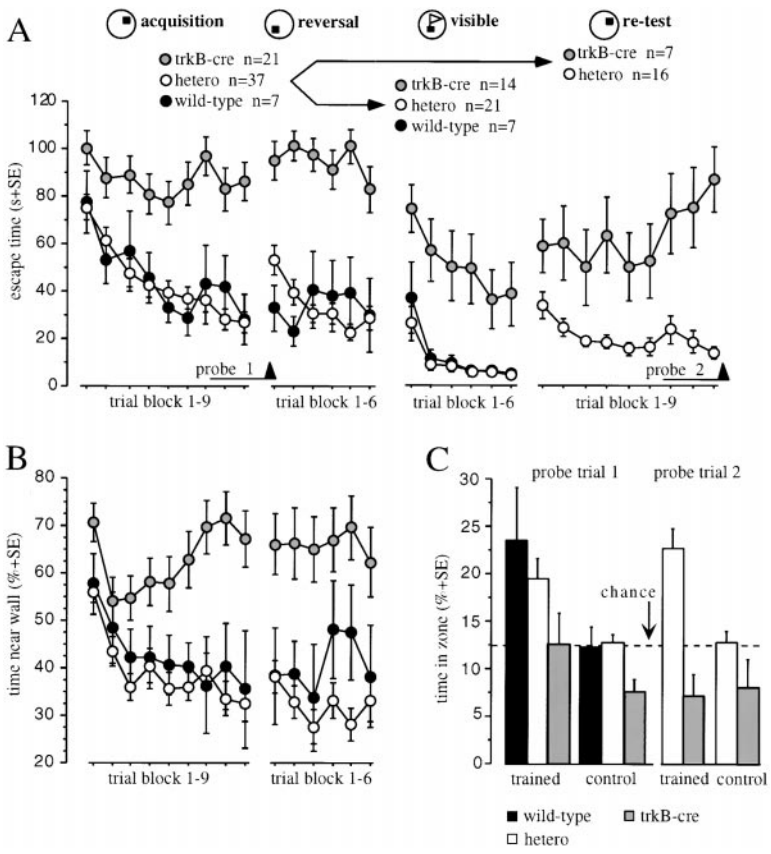

Figure 5. Impaired Learning of *trkB*–CRE Mice in Spatial Memory Tasks—Morris Water Maze

(A) Acquisition phase during invisible and visible (cued) version. Mice were trained for 18 trials (trial block 1–9) spread over 3 consecutive days (six trials per day) in the invisible version, followed by 2 days of reversal phase with the platform at the opposite position in the pool. Groups were split as indicated for the visible version and for additional training in the invisible version (retest). Escape latency is expressed in seconds required to find the platform.

(B) Wall hugging behavior (thigmotaxis) during acquisition and reversal phase, expressed as percentage of swim time spent in a rim of 22.5 cm from the walls. (C) Probe trials (indicated in [A]) expressed as percent time spent in a circular zone around the former goal or control zone. Chance level (12.5%) is indicated as stippled line. *trkB*–CRE mice are complete nonlearners in all aspects of Morris water maze training. Performance of *trkB*–CRE mice in the visible test did improve over time. However, performance remained poor compared to controls even after extended training and when assayed in experimentally naive mice (data not shown).

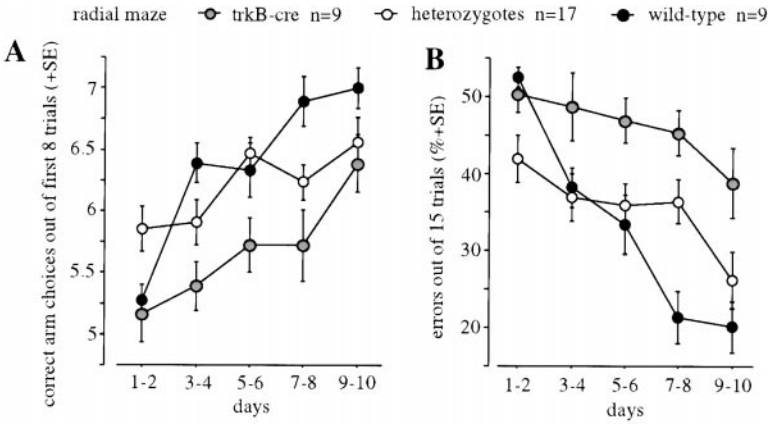

Figure 6. Partial Failure of *trkB*–CRE Mice in the Eight-Arm Radial Maze

Mice were trained for 10 consecutive days in the eight-arm fully baited radial maze. Learning performance is expressed as (A) the mean number of correct arm choices from the first eight trials, a measure of spatial working memory, and (B) the percentage of errors until eight correct choices have been observed or after the maximal permitted number of trials (15), a measure reflecting inappropriate search strategies. The performance of $trkB^{lox/+}$ mice (wild-type) was statistically indistinguishable from heterozygotes, whereas the performance of *trkB*–CRE mice was significantly impaired compared to control and heterozygotes (see text).

dark compartment, before being returned to their home cage. Before the shock, all groups of mice showed similar short step-through latencies (Figure 7A). The test after 24 hr showed that all groups including *trkB*–CRE mice had learned to avoid the dark compartment, as indicated by a much increased step-through latency (Figure 7A). A more complicated test to assess fear-related passivity uses the immobility ("freezing") reaction of mice in response to repeated high-intensity foot shocks paired with a tone. The mutant mice showed retarded acquisition of the freezing response during the shocks, lack of freezing when placed in the box after 30 min (contextual response), but normal freezing to context after 24 and 72 hr. Yet, freezing to tone in a different environment was impaired (data not shown).

We next tested the mice in an active avoidance test, in which mice are placed in a two-chamber ("shuttle") box and taught to avoid a signaled electric shock (unconditioned stimulus [US]) by running into the opposite compartment (Büeler et al., 1992). The shock is preceded by a warning light (conditioned stimulus [CS]). In this test, all groups showed a distinct learning curve (Figure 7D), the two-way avoidance learning of *trkB*–CRE mice being slightly facilitated compared to controls ($P = 0.012$). Upon first exposure to the shuttle box, the mutants showed the same activity level as the controls. After having received the first shocks, however, the *trkB*–CRE mutants developed, in comparison to control mice, a persisting locomotor activity ($P < 0.0001$). The locomotor activity levels (both prior and within sessions) increased over days, implying that the observed superior learning was a function of increased locomotor activity as often observed after lesions of the rodent hippocampus (Jarrard, 1976; O'Keefe and Nadel, 1978), while the learning of the controls was not associated with gross changes in locomotor activity (Figures 7B and 7C). Both groups very rarely failed to escape the shock, indicating that their shock sensitivity was similar. In summary, a certain degree of task-specific long-term memory appears to be present in the *trkB*–CRE mutants, but they show increasingly impaired learning behavior or inappropriate coping responses when facing complex and/or stressful learning paradigms such as in contextual fear conditioning, two-way avoidance, radial maze, and water maze learning.

trkB–CRE Mice Show Reduced Hippocampal Long-Term Potentiation

Defective spatial learning often correlates with impaired long-term potentiation (LTP) in the hippocampus (Chen and Tonegawa, 1997), which has led to the view that LTP is a good model for cellular changes occurring in learning and memory (Bliss and Collingridge, 1993). To test if the behavioral abnormalities seen in *trkB*–CRE mice were associated with changes in LTP, we measured CA3–CA1 LTP in hippocampal slices after theta burst stimulation (TBS) with 100 Hz (see the Experimental Procedures). An experiment was classified as "successful LTP" when the average of the EPSP slope size 55–60 min after TBS showed an increase of at least 20% above baseline values. Whereas mice wild-type for TrkB protein ($trkB^{lox/+}$) showed LTP in 83% of all cases, heterozygotes and *trkB*–CRE mice were impaired and showed only LTP in 48.5% and 37% of the cases, respectively (Figure 8A). In addition, the magnitude of the potentiation was different between wild-type and mutants. The mean EPSP slope as percentage of baseline 55–60 min

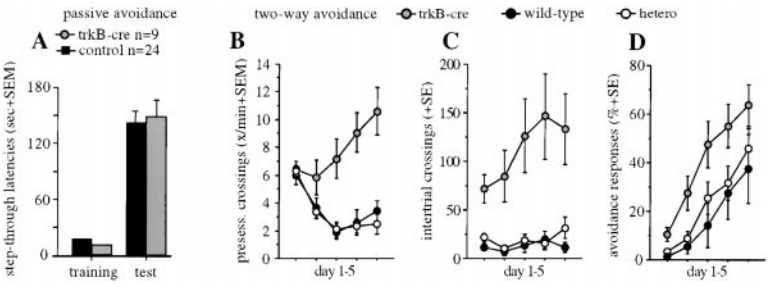

Figure 7. Normal Learning of *trkB*–CRE Mice in Simple Passive Avoidance and Maladaptative Improvement of Two-Way Avoidance Learning

(A) Passive (one-trial inhibitory) avoidance. Mice were tested for step-through latencies into the dark compartment before (training) and after foot shock (test). (B–D) Two-way active avoidance. Mice were trained for 5 days, 80 trials per day. Number of crossings into opposite compartment during presession (B) and between trials (C). (D) Percentage of correct responses (avoidance of the shock). Note that spontaneous presession activity and intertrial activity was massively increased in *trkB*–CRE mice as compared to control mice ($P = 0.0001$), the latter learning the response without increasing locomotor activity.

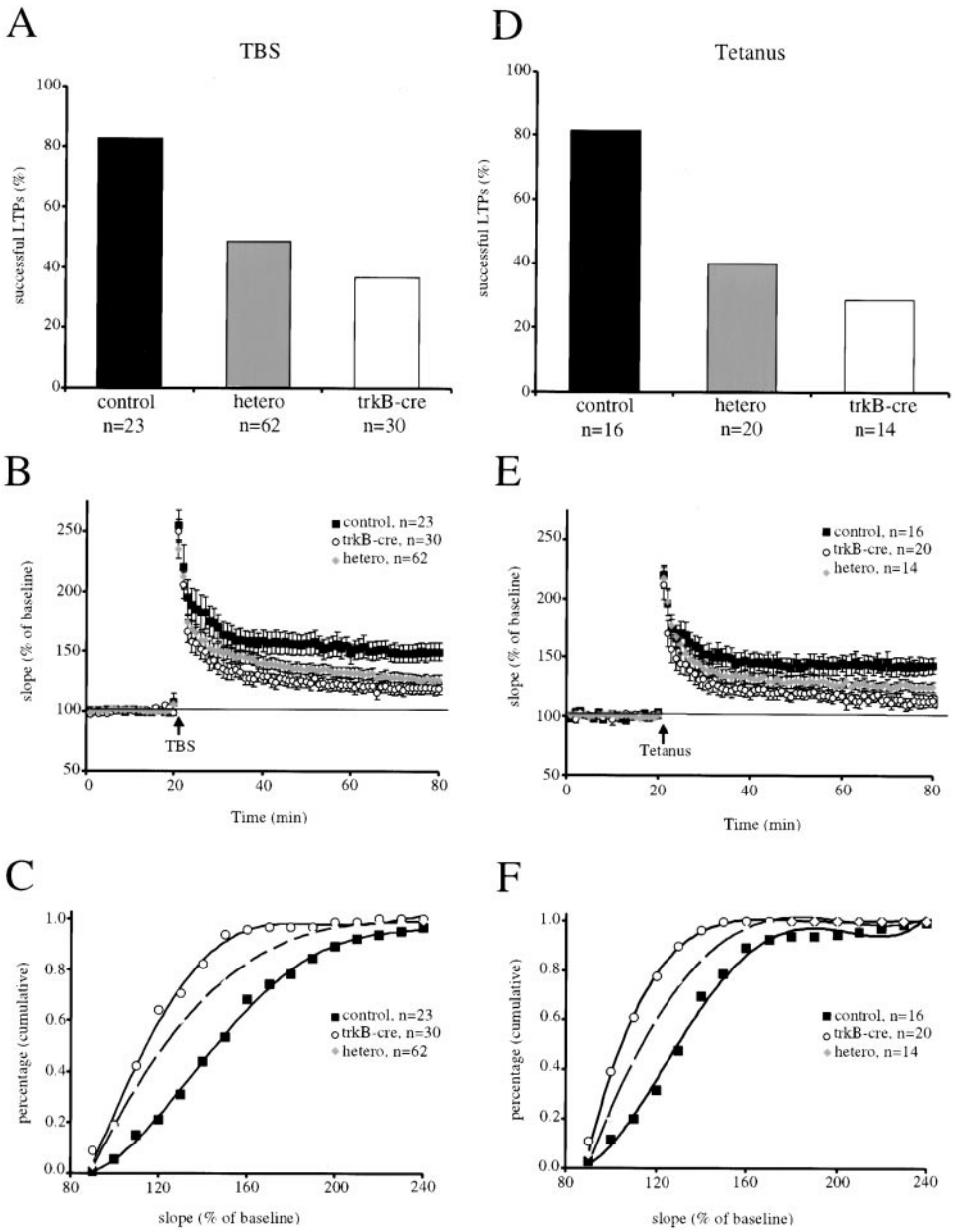

Figure 8. Reduced Synaptic Plasticity in the Hippocampus of *trkB*–CRE Mice

(A–C) Data from theta burst stimulation (TBS). (D–F) Data from tetanus stimulation protocol. The TBS protocol was applied to three control mice, nine heterozygous mice, and four *trkB*–CRE mice; the tetanus protocol was applied to four mice per genotype; n equals number of slices.

(A and D) Percentage of successful LTP inductions for all genotypes. LTP was judged as successful if 55–60 min after the TBS or tetanus the slope of the field EPSP was greater than 120% of the baseline value (baseline = 100%). Group data for $trkB^{lox/null}$ and $trkB^{lox/+}$;CaMKII–CRE animals are combined (heterozygotes).

(B and E) Group data for field EPSP recordings before and after TBS or tetanus application. This combination of group data shows that *trkB* mutant mice show an equally diminished potentiation after TBS or tetanus stimulation. Error bars, SEM. The difference between wild-type and *trkB*–CRE or heterozygotes is significant for TBS ($p = 0.003$, t-test, two-tailed) and for tetanus stimulation ($p = 0.005$). The difference between heterozygotes and *trkB*–CRE mice is also significantly different for TBS ($p = 0.03$) and for tetanus stimulation ($p = 0.04$).

(C and F) Cumulative percentage distribution of field-EPSP slopes, expressed as percentage of baseline values. All data points recorded between 30–60 min after application of the TBS or tetanus are included. The ordinate gives the fraction of the data points that exhibit a posttetanic field-EPSP slope less or equal to the value shown on the abscissa. The curves very quickly reach 100% for heterozygotes and *trkB*–CRE mice, indicating that only a minority of the slices show a substantial potentiation. In contrast, slices from wild-type mice only reach the 100% late, i.e., many of them show strong potentiation. For both stimulation protocols, heterozygous and *trkB*–CRE mice show a significant difference.

after stimulation was 149.1 ± 7.5% (n = 23 slices) for wild-type, 126.9 ± 5.9% (n = 62) for heterozygotes, and 119.3 ± 5.1% (n = 30) for *trkB*–CRE mice (see Figure 8B). The difference between wild-type and mutants ($P = 0.003$; two-tailed t-test) and the difference between heterozygotes and *trkB*–CRE mice ($P = 0.02$) were significant. Especially in the first 40 min of recording after TBS, heterozygotes show a higher amount of potentiation in comparison to *trkB*–CRE mice, whereas the difference at 60 min is also significant but much smaller (Figure 8B). It is noteworthy that mutant animals show a slow decline of their already small LTP over time (see, e.g., the last 40 min of recording in Figure 8B). This might indicate that even in those animals in which LTP can be induced, a later phase of LTP is significantly affected. Figure 8C shows the cumulative distribution of synaptic enhancements 30 to 60 min after TBS for all animal types. These distributions show that in wild-type mice the enhancement in most cases is greater than 140%, whereas the enhancement for heterozygotes and *trkB*–CRE mice in only a few cases substantially differed from 100%. The distribution of heterozygous and *trkB*–CRE mice is also different: heterozygous show more data points with a higher potentiation on average. Similar results were obtained when LTP was induced using tetanus stimulation (Figures 8D, 8E, and 8F), indicating that the impairments in LTP in both heterozygotes and *trkB*–CRE mice were not specific to theta burst stimulation. It is important to point out that also for tetanus stimulation, heterozygous and *trkB*–CRE mice are significantly different ($p < 0.05$, t-test, two-tailed, Figures 8E and 8F).

Normal Basal Synaptic Transmission in *trkB*–CRE Mice

A number of control experiments indicated that the failure to induce LTP in mutant mice was not merely due to impaired synaptic transmission. According to our tests, synaptic transmission in mutant mice was indistinguishable from that in wild-type mice in many ways. First, we compared the size of the presynaptic fiber volley (PSFV), which is proportional to the number of presynaptic neurons recruited by stimulation, with the slope of the field EPSP to provide an accurate indication of basal synaptic transmission. By these means, we found that basal synaptic transmission was normal in *trkB*–CRE and heterozygous mice: *trkB*–CRE (ratio EPSP slope/PSFV), 2.3 ± 0.46; heterozgyous, 2.5 ± 0.3; control, 2.7 ± 0.37. (all P values > 0.1, t-test, two-sided). Secondly, paired pulse facilitation (PPF) was normal in all animal types, measured for interstimulus interval (ISI) from 10 to 160 ms (Figure 9A). Even if the induction of LTP failed, all slices showed posttetanic potentiation (PTP) when the TBS or the tetanus was applied (see Figure 8).

To specifically test if NMDA receptor transmission was affected in *trkB*–CRE mice, we measured the NMDA receptor component of the EPSP under low Mg^{2+} condition. In the presence of the AMPA receptor antagonist DNQX, slices from mutant mice showed a NMDA receptor component of the EPSP comparable to control mice. The reduction of the signal was 71.1 ± 6.8% in *trkB*–CRE mice, compared to 70.5 ± 4.3% in control and 72.1 ± 5.2% in heterozygous mice (Figures 9B and 9C). There was no statistical difference between all three genotypes ($p > 0.1$, t-test). This NMDA component of the field EPSP was in all cases reduced to zero when the NMDA receptor antagonist AP-5 was added.

To test if the impaired LTP was due to impaired fiber function or to altered release probabilities of CA3 axon terminals, we analyzed the EPSP slope during theta burst stimulation (Figures 9D–9F). Synaptic fatigue during high-frequency stimulation was observed in all genotypes. To quantitate this effect, we compared the fourth response in relation to the first response in a burst of four stimuli (one burst consists of four stimuli with 100 Hz, given 10 times with an interstimulus interval of 200 ms) and calculated this ratio for all three theta bursts given. There was no statistically significant difference between all genotypes ($p > 0.1$, t-test). In summary, our electrophysiological experiments revealed normal synaptic transmission but impaired synaptic strengthening in heterozygous and *trkB*–CRE mice.

Discussion

Here, we have shown that the TrkB receptor tyrosine kinase is an essential component of the protein kinase cascades regulating synaptic plasticity and behavior. Because the behavioral changes are associated with strongly reduced expression of TrkB across most forebrain structures, sparing inhibitory interneurons, there is no satisfactory lesion model of single structures explaining the observed behavioral changes. The best description would be that of a moderate “hippocampal plus” lesion syndrome, as the behavioral effects include many features of hippocampal lesion such as strong deficits in water maze including the cued version (Logue et al., 1997), moderate ones in the radial maze (Ammassari-Teule and Passino, 1997), improved two-way avoidance (O’Keefe and Nadel, 1978), persistent thigmotaxis (Hostetter and Thomas, 1967), and missing habituation (Misslin et al., 1981). These appear to be combined with (or reinforced by) partial impairments of the amygdala as reflected in impaired water maze (Packard and Teather, 1998), radial maze learning (Rossi-Arnaud and Ammassari-Teule, 1998), and impaired fear conditioning to tone (Phillips and Ledoux, 1992). Likewise, lesions of the prefrontal (Compton et al., 1997; de Bruin et al., 1997) and entorhinal cortex (Nagahara et al., 1995; Kirkby and Higgins, 1998) are known to affect different components of swimming navigation learning, to impair radial maze learning (Ammassari-Teule and Passino, 1997), and to interfere with selection of motor strategies and behavioral flexibility (Lipska et al., 1994; Compton et al., 1997). The contribution of TrkB-induced striatal hypofunction is difficult to evaluate, as striatal functions are intimately linked to the functions of the overlying cortical regions, forming a portion of the cortico-subcortical parallel loop system comprising the associative cortex and limbic cortex, ventral striatum, ventral tegmentum, hypothalamus, reticular formation, and limbic and intralaminar thalamus, which ultimately regulates cognitive processing in mammals (Lipp and Wolfer, 1998). It remains to be seen whether the missing deficit of the *trkB*–CRE mutants in passive avoidance indicates some degree of sparing of hippocampus or other structures mentioned above or whether it reflects the simplicity of the task that makes it suitable for compensatory mechanisms.

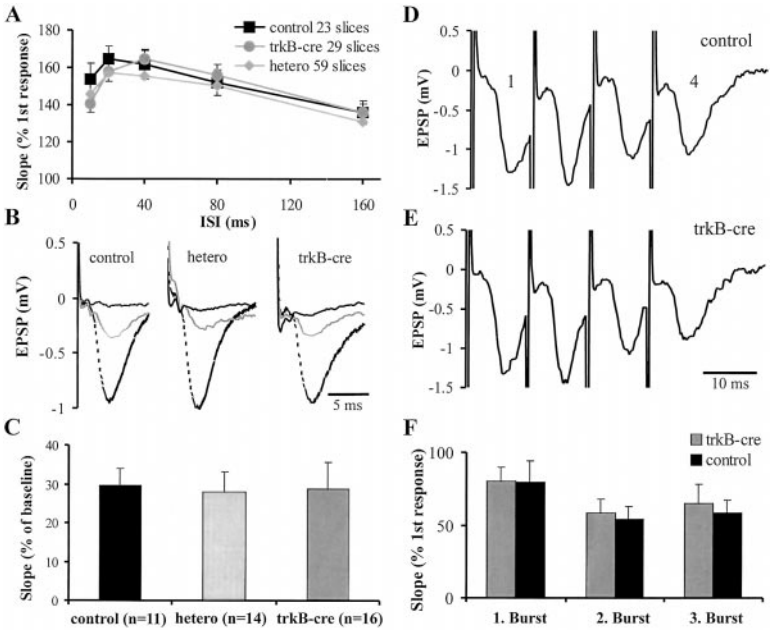

Figure 9. Normal Basal Synaptic Transmission in *trkB*–CRE Mice

(A) Paired pulse facilitation (PPF) was measured to determine whether this aspect of synaptic transmission was normal in *trkB*–CRE mice compared to wild-type control slices. The percentages denote the ratio of the second EPSP-slope to the first EPSP-slope. PPF was tested with 10, 20, 40, 80, and 160 ms interstimulus interval (ISI). There is no significant difference between all genotypes. Error bars, SEM.

(B) AMPA receptor (DNQX) and NMDA receptor antagonists (AP-5) were used to analyze whether NMDA receptors are functional in *trkB*–CRE mice. Shown are single traces for all genotypes, extracellular recording. Dashed line, baseline EPSP; gray line, 15 min after DNQX application; black line, 15 min after AP-5 + DNQX application.

(C) Summary data for all pharmacological experiments. Plotted is the ratio of the EPSP slope 15 min after DNQX application in comparison to baseline recordings. Error bars, SEM; n, number of slices. There is no statistically significant difference between all genotypes ($p > 0.1$, t-test).

(D–F) Synaptic fatigue during high-frequency stimulation. Single trace during theta burst stimulation of a $trkB^{lox/+}$ (control) animal (D) and a *trkB*–CRE mouse (E). Response to the fourth stimulus (indicated with "4") was compared to the first stimulus (indicated with "1"). (F) Group data for all control and *trkB*–CRE animals. Plotted is the ratio of the fourth response to a burst of four stimuli during theta burst stimulation in comparison to the first response. For LTP induction, three theta bursts were applied, and data are shown for all three bursts. Synaptic fatigue can be observed in all genotypes, but there is no statistically significant difference between control, heterozygous (data not shown), and *trkB*–CRE mice ($p > 0.1$ t-test).

In any event, one may note that passive avoidance performance is in many cases not affected by hippocampal lesions (O'Keefe and Nadel, 1978). Likewise, the occurrence of freezing responses to contextual cues in hippocampally lesioned mice is strain dependent (Logue et al., 1997). Thus, the lack of a deficit as observed here does not necessarily indicate sparing of the hippocampus.

It appears that procedural long-term memory (how to do it) and sensory memory is relatively spared in the *trkB*–CRE mutants as evidenced by clear learning across several tasks. On the other hand, the problem of these mice seems to be the impaired short-term adaptation of behavior as soon as the task gets difficult or stressful. This may even prevent acquisition of a particular task. For example, the persistent thigmotaxis in the water maze does clearly prevent learning of this task, making it impossible to determine whether or not the *trkB*–CRE mutants have a spatial memory deficit. In the radial maze, the mice accumulate perseverative errors at the end of the task when it is getting difficult. However, the learning curve indicates that long-term memory must be present. This can also be observed in contextual fear conditioning in which the mutants fail to develop an appropriate freezing response after 30 min but show correct freezing after 24 hr yet not following exposure to tone. Lastly, the data from avoidance learning point into the same direction, as the *trkB*–CRE mutants first reacted normally to the new environment but fell into a persisting (and, for mice who normally become passive) maladaptative locomotor activity. Taken together, the observed behavioral deficits point toward a deficit in synaptic short-term plasticity within the hippocampus and its proximally connected forebrain structures, most likely including the anterior and intralaminar nuclei (Mair et al., 1998). While specific memories appear to be partially conserved, one would expect that the dyscoordination syndrome characteristic for the *trkB*–CRE mutants should result in loss of episodic memory, as this requires encoding and retrieval of modality-specific sensory and motor memories coordinated by the hippocampus (Eichenbaum et al., 1999; Lisman, 1999). Assessing episodic memory in *trkB* mutant mice will require, however, the development of new behavioral tests.

The only significant morphological alteration that was found in *trkB*–CRE mice was a mild reduction in myelinated axons in the hippocampus that may occur to a similar degree elsewhere in the brain. This defect is unlikely to produce general hippocampal dysfunction, since all basal synaptic parameters were found to be normal in all genotypes. Heterozygous mice, which show no reduction in myelinated axons, display markedly reduced LTP (see below), indicating that other functions of TrkB are responsible for long-term synaptic enhancement. Finally, even severely demyelinated animals such as mutants carrying *shiverer* alleles apparently show normal learning behavior in the radial maze (Inagawa et al., 1988). As discussed by Cellerino et al. (1997), BDNF may exert trophic functions on CNS neurons thereby affecting cell and axon size. In the absence of BDNF/TrkB signaling, axonal diameters may be somewhat reduced resulting in hypomyelination of the smallest caliber axons.

Our electrophysiological experiments confirmed previous studies that had indicated an important role for the endogenous BNDF/TrkB system in hippocampal long-term potentiation (Shieh and Ghosh, 1997). The overall deficit in synaptic strengthening is very similar to that

observed in *BDNF* null mice (Korte et al., 1995; Patterson et al., 1996; Pozzo-Miller et al., 1999), although the deficit in heterozygous and homozygous mutant *BDNF* null mice was somewhat stronger compared to the deficits in heterozygous and homozygous *trkB*–CRE mice, respectively. It is possible that the levels of BDNF protein are more limiting than those of the receptor. In the case of *trkB*–CRE mice, one should keep in mind that a small percentage of TrkB protein remained and may represent a small fraction of pyramidal neurons with an unrecombined trkB locus. Using an independently generated floxed trkB allele, L. F. Reichardt and colleagues have also observed impaired CA3–CA1 hippocampal LTP as a consequence of reducing TrkB protein levels (L. F. Reichardt, personal communication).

An interesting point is the dissociation between LTP impairment in the heterozygous animals and the lack of behavioral deficits in those mice. Pending confirmation that the heterozygotes do not show undetected minor behavioral deficits, and measurements of LTP in vivo, we conclude that a 50% reduced rate of LTP at 100 Hz and a significant reduction of EPSP slope size compared to wild-type mice after TBS or tetanus application does not necessarily translate into defects in learning and memory. Two interpretations seem plausible. Spatial learning may not require hippocampal CA3/CA1 LTP. Support for this conclusion comes from a number of studies in which impairments in hippocampal LTP were not associated with spatial learning deficits (Bannerman et al., 1995; Nosten-Bertrand et al., 1996; Okabe et al., 1998). Alternatively, the precise strength of hippocampal LTP may be critical for spatial learning to occur. Excessive LTP as observed in mutant mice lacking the GluR2 receptor (Gerlai et al., 1998) or the postsynaptic density protein PSD-95 (Migaud et al., 1998) is correlated with behavioral impairments. Reduced LTP as observed in *trkB*–CRE mice might be below the critical threshold and also translates into impaired learning, while the reduction in LTP in heterozygous trkB mutants would be sufficient for spatial learning. Complex spatial learning may therefore depend on a precisely tuned critical bandwidth of LTP.

Basal synaptic parameters appear to be completely normal in *trkB*–CRE mice. These findings are perfectly in line with a previous study on BDNF knockout mice (Korte et al., 1995). However, they differ from another study using an independently generated BDNF knockout line (Patterson et al., 1996). In this latter study, paired pulse facilitation was impaired and EPSP size was smaller in comparison to wild-type mice. In a more recent study, using BDNF knockout mice (Pozzo-Miller et al., 1999), it was shown that synaptic fatigue is somewhat larger in the mutants, probably due to the fact that the number of vesicles docked at presynaptic active zones is reduced. We did not observe any changes in synaptic fatigue during high-frequency stimulation. The fact that *trkB* null mutants but not *trkB*–CRE mice show abnormal synapse morphology (Martinez et al., 1998) suggests that the discrepancies in basal synaptic parameters may at least in part be due to developmental defects in the null mutants.

Currently, the mechanisms by which BDNF/TrkB regulate synaptic strength are poorly understood. There is evidence that TrkB signaling is important in the presynaptic neuron to regulate neurotransmitter release (Lessmann et al., 1994; Li et al., 1998) and to control the complexity of presynaptic arbors (Cohen-Cory and Fraser, 1995; Inoue and Sanes, 1997). In addition, TrkB signaling may be important in postsynaptic dendrites, either by promoting or inhibiting dendritic growth or by modifying neurotransmitter receptor activity (see recent review by McAllister et al. [1999]). N-methyl-D-aspartate (NMDA) receptor channels are essential for hippocampal-dependent learning and memory (Chen and Tonegawa, 1997), and NMDA receptor-mediated currents are enhanced by tyrosine phosphorylation (Yu et al., 1997), which could in part result from TrkB signaling (Levine et al., 1998). We did not observe an overall reduction in steady-state NMDA receptor subunit tyrosine phosphorylation in the hippocampus of *trkB*–CRE mice (unpublished data). However, tyrosine phosphorylation of NMDA receptors may be transient and limited to active processes during LTP. The intracellular pathways downstream of TrkB receptors that regulate synaptic function are unknown. TrkB receptor activation at synapses may lead to the activation of the Fyn tyrosine kinase (Iwasaki et al., 1998), the MAP kinase pathway (Kaplan and Miller, 1997), and the CREB transcription factor (Finkbeiner et al., 1997), all of which are strongly implicated in LTP and learning (Milner et al., 1998).

Taken together, this study, in which TrkB has been eliminated to a large extent from the forebrain, indicates an essential role for TrkB neurotrophin receptor signaling in complex learning and synaptic plasticity mediated by the hippocampus and its proximally connected forebrain structures. Future work in which CRE-mediated recombination will be further restricted to subregions of the forebrain, to either the presynaptic or postsynaptic neuron, or regulated in time, will shed light on the mechanisms and on neuronal pathways that require TrkB signaling during learning and memory formation.

Experimental Procedures

Transgenic Animals

The generation of the floxed *trkB* allele was done by homologous recombination in embryonic stem (ES) cells according to standard protocols (Klein et al., 1993). The expression vector for CaMKII–CRE transgenic mice consists of the 8.5 kb CaMKIIα promoter (Mayford et al., 1996) followed by a hybrid intron in front of the CRE coding region with nuclear localization sequence and a SV40 polyadenylation signal. Transgenic line CaMKII–CRE-159 was generated as described (Hogan et al., 1994). Southern blot analysis of recombination of the loxP-flanked betaT14 allele (Gu et al., 1994) revealed for CaMKII–CRE-159 at an age of 8 weeks about 50% recombination in hippocampus, cortex, and olfactory bulb, but no deletion in cerebellum, liver, kidney, spleen, or tail (data not shown). The mice used for this study were kept on a C57Bl/6 genetic background (60%) with contributions of 129/sv and CBA/J from the Flp and CRE transgenic crosses. Phenotypic analyses of mutant mice on different genetic backgrounds were not done, since previous analyses of *trkB* null mutants had revealed no changes in phenotype when backcrossed to other inbred and outbred strains (L. M. and R. K., unpublished data).

Biochemistry

Mice were killed by cervical dislocation, and various regions of the mouse brain were quickly dissected and frozen in liquid nitrogen. Cell lysates from tissues were homogenized in lysis buffer (50 mM Tris [pH 7.5], 120 mM NaCl, 1% Triton X-100, 1 mM sodium orthovanadate, 10 mM NaF, and 1 mM NaPP) and protease inhibitors (10 μg/ml leupeptin, 2 μg/ml aprotinin, 5 mM benzamidin, and 1 mM PMSF) and centrifuged at 4°C to remove insoluble material. Samples

were incubated with specific antibodies, and products were analyzed as previously described (Minichiello et al., 1998). Relative levels of TrkB protein were quantified from ECL stained immunoblots using the NIH Image program.

Histology and Electron Microscopy

Histological and immunohistochemical analyses were carried out as described (Minichiello and Klein, 1996). Monoclonal antibodies against 200 kDa neurofilament (clone RT97), MAP2 (clone AP20) (Boehringer, 1:200 and 1:300, respectively), calbindin, parvalbumin (Sigma; 1:400 and 1:1000, respectively), and polyclonal antibody directed against CRE recombinase (Kellendonk et al., 1999) were used. Immunoreactivities were detected using peroxidase Vector Kit, fluorescein (DTAF)- or rhodamine-conjugated secondary anti-mouse antibody, or fluorescein (FITC)-conjugated secondary anti-rabbit (Jackson, 1:200). Nissl and Golgi stains were done according to standard procedures. Staining for β-galactosidase using X-gal was done on 20–35 μm sections as described (Tsien et al., 1996). Electron microscopic analyses were done on perfused brains (1.5% glutaraldehyde,1.5% paraformaldehyde, and 2.5% polyvinylpyrrolidone, in phosphate buffer [pH 7.3]) postfixed in 1% OsO_4/1.5% potassium hexanoferrate, rinsed in 0.1 M cacodylate buffer and 0.2 M sodium maleate buffer (pH 6.0), and block stained with 1% uranyl acetate. Fifty nanometer sections were examined with a Zeiss EM10. Counts of myelinated axons were made at a magnification of 4,300× in the strata pyramidale and radiatum of the CA1 region over a total area varying from 177,419 to 338,709 μm^2 per hippocampus.

Behavioral Tests

Behavioral tests were performed as previously described using littermates of 9–16 weeks of age (Büeler et al., 1992; Müller et al., 1994). Locomotor abilities were assessed by a variety of measures in the behavioral tests below, none of which yielded impairments in the *trkB* mice (data not shown). For two-way avoidance test, mice were placed in sound-proof computer-operated shuttle boxes (Campden Instruments). After 2 min during which mice were left undisturbed (presession), conditioning light stimulus lasting 5 sec was delivered and followed by 10 sec electric shock of 0.15 mA of intensity. Intertrial interval varied between 5 and 15 sec. The animals performed 80 trials a day for 5 days.

For the one-trial inhibitory avoidance, mice were trained in an apparatus in which a straight alley was divided into two compartments. The smaller compartment was made of white Plexiglas. The larger one was made of black Plexiglas and was equipped with a removable cover of the same material to allow the compartment to be in darkness. A tensor lamp illuminated the small compartment. The floor of the larger compartment consisted of two oblique stainless steel plates folded at the bottom through which a constant current could be delivered. On the training day, each mouse was placed in the lit compartment, facing away from the dark compartment. When the mouse had stepped with all four paws into the dark side, the door was closed, the step-through latency was recorded, and two foot shocks (0.4 mA, 50 Hz, 2 sec) were delivered with an interval of 5 sec. The maximum initial step-through latency allowed as a criterion for the animals entering the trial was 15 sec. The mouse was then removed from the apparatus and returned to its home cage. Retention was tested 24 hr later following a similar procedure, except that no shock was administered. A maximum step-through latency of 180 sec was allowed in the test session.

The Morris navigation test was carried out in an open-field water maze of 1.5 m in diameter and filled with opaque water at the temperature of 25 ± 1°C, located in a laboratory that contained prominent extramaze cues. A hidden 15 cm diameter platform was used. Trials lasted a maximum of 120 sec. Spatial training consisted of 18 trials (6 per day, separated by an interval of about 30 min) during which the platform was left in the same position. After 3 days of learning, the platform was moved to the opposite position, and reversal learning was monitored for 2 additional days (six trials per day). For additional testing of subgroups, see text.

For the radial maze test, the animals were singly housed with water provided ad libitum. Mice were gradually reduced to 85% of their free-feeding body weight and, throughout the experiment, they were maintained at their reduced weights by being fed a premeasured amount of chow each day. The apparatus was a gray plastic maze with eight identical arms radiating 37 cm from an octagonal starting platform (perimeter, 7 × 8 cm), in which mice run freely. All eight arms were baited with a 20 mg food pellet at the beginning of each session, and the baits were not replaced. Animals received one trial per day; each daily trial terminated when 8 correct choices were made (maximum 15 choices) or 15 min had elapsed. An arm choice was defined as placement of all paws on a maze arm. An error was committed when an animal entered a previously visited arm.

Electrophysiology

Hippocampal transverse slices (400 μm thick) were prepared and maintained using standard procedures (medium: 124 mM NaCl, 3 mM KCl, 1.25 mM KH_2PO_4, 2 mM Mg_2SO_4, 26 mM $NaHCO_3$, 2.5 mM $CaCl_2$, and 10 mM glucose; temperature 32 ± 0.2°C; submerged recording). Monopolar tungsten electrodes in the CA3 Schaffer-collateral region were used for stimulation. Synaptic field potentials were elicited with a frequency of 0.1 Hz. Responses were recorded with glass electrodes placed in the apical dendritic region (stratum radiatum) of the CA1 pyramidal neurons. The slope of the EPSP was calculated and used as a measure for synaptic strength. LTP was induced with a theta burst stimulation (TBS) of 10 bursts with four pulses each (100 Hz, 100 μs duration, 200 ms interburst interval) with the strength of the test stimulus; this TBS was repeated three times with an ISI of 10 sec. Data were collected with a program written in LabView (National Instruments). Alternatively, LTP was induced with a tetanus of 3 × 30 pulses (100 Hz, 100 μs duration, 5 sec ISI) with the strength of the test stimulus. Routinely paired pulse facilitation (PPF) was tested, with 10, 20, 40, 80, and 160 ms ISI. An experiment was classified as "successful LTP" when the average of the EPSP slope size 55–60 min after TBS showed an increase of at least 20% in comparison to baseline values. Data for the two different heterozygous $trkB^{lox/+}$;CaMKII–CRE and $trkB^{lox/null}$ mice were pooled, because they showed no significant difference in LTP size, successful induction of LTP, or PPF (in all cases t-test, two-tailed, $p > 0.1$). All measurements were carried out and analyzed in a strictly blind fashion—the distribution of the slices into the incubation chamber was done by a second experimenter so that the investigator performing the measurements had no way of telling from which type of slice he was recording. Additionally, the genotype of all animals was only revealed after the electrophysiological experiments and their evaluation. On each experimental day, two mice from the same litter were tested.

Pharmacology: after 30 min baseline recording, DNQX (DNQX = 6,7-dinitroquinoxaline 2,3-dione, 10 μM) in low Mg^{2+} (1 mM) ACSF was applied via the bath. After 20 min, AP-5 (DL-2-amino-5-phosphonovalerate, 50 μM) together with DNQX were applied for 30 min to the same slice.

Acknowledgments

We acknowledge excellent technical assistance from B. Brühl (University Heidelberg), V. Staiger (Max-Planck Institute), A. Vyssotski (University of Zürich), F. Diella, A. Renvaktar, the European Molecular Biology Laboratory transgenic service and animal house, and Reiner Saffrich for help in generating the image overlays. We also thank B. Xu and L. F. Reichardt, who have independently generated a floxed *trkB* mouse, for communication of results prior to publication and for helpful comments; C. Kellendonk and G. Schütz for the CRE rabbit antiserum, F. Stewart and P. Orban for plasmids, A. Berns for lox-lacZ reporter mice, and A. Oliverio, R. G. M. Morris, P. Seeburg, R. Brambilla, and P. Orban for helpful comments on the manuscript. This work was in part supported by the Max-Planck Society (to T. B. and M. K.) and by grants from the Volkswagen foundation (to R. Kühn and R. Klein), from the Deutsche Forschungsgemeinschaft SFB 317, from two European Union Biotechnology Network Grants (to R. Klein and H.-P. L.), and from the Swiss National Science Foundation (to H.-P. L.) and the EMDO foundation Zürich (to D. P. W.).

Received June 29, 1999; revised July 12, 1999.

References

Akagi, K., Sandig, V., Vooijs, M., Van der Valk, M., Giovannini, M., Strauss, M., and Berns, A. (1997). Cre-mediated somatic site-specific recombination in mice. Nucleic Acids Res. *25*, 1766–1773.

Alcantara, S., Frisen, J., del Rio, J.A., Soriano, E., Barbacid, M., and Silos-Santiago, I. (1997). TrkB signaling is required for postnatal survival of CNS neurons and protects hippocampal and motor neurons from axotomy-induced cell death. J. Neurosci. *17*, 3623–3633.

Ammassari-Teule, M., and Passino, E. (1997). The dorsal hippocampus is selectively involved in the processing of spatial information even in mice with a genetic hippocampal dysfunction. Psychobiology *25*, 118–125.

Bannerman, D.M., Good, M.A., Butcher, S.P., Ramsay, M., and Morris, R.G. (1995). Distinct components of spatial learning revealed by prior training and NMDA receptor blockade. Nature *378*, 182–186.

Barbacid, M. (1995). Neurotrophic factors and their receptors. Curr. Opin. Cell Biol. *7*, 148–155.

Bliss, T.V.P., and Collingridge, G.L. (1993). A synaptic model of memory: long-term potentiation in the hippocampus. Nature *361*, 31–39.

Büeler, H., Fischer, M., Lang, Y., Bluethmann, H., Lipp, H.-P., DeArmand, S.J., Prusiner, S.B., Aguet, M., and Weissmann, C. (1992). Normal development and behaviour of mice lacking the neuronal cell-surface PrP protein. Nature *356*, 577–582.

Cahill, L., and McGaugh, J.L. (1990). Amygdaloid complex lesions differentially affect retention of tasks using appetitive and aversive reinforcement. Behav. Neurosci. *104*, 532–543.

Cellerino, A., Carroll, P., Thoenen, H., and Barde, Y.-A. (1997). Reduced size of retinal ganglion cell axons and hypomyelination in mice lacking brain-derived neurotrophic factor. Mol. Cell. Neurosci. *9*, 397–408.

Chen, C., and Tonegawa, S. (1997). Molecular genetic analysis of synaptic plasticity, activity-dependent neural development, learning and memory in the mammalian brain. Annu. Rev. Neurosci. *20*, 157–184.

Cohen-Cory, S., and Fraser, S.E. (1995). Effects of brain-derived neurotrophic factor on optic axon branching and remodeling in vivo. Nature *378*, 192–196.

Compton, D.M., Griffith, H.R., McDaniel, W.F., Foster, R.A., and Davis, B.K. (1997). The flexible use of multiple cue relationships in spatial navigation: a comparison of water maze performance following hippocampal, medial septal, prefrontal cortex, or posterior parietal cortex lesions. Neurobiol. Learn. Mem. *68*, 117–132.

Davies, A.M. (1997). Neurotrophins: the yin and yang of nerve growth factor. Curr. Biol. *7*, R38–R40.

Davies, A.M., Minichiello, L., and Klein, R. (1995). Developmental changes in NT3 signaling via TrkA and TrkB in embryonic neurons. EMBO J. *14*, 4482–4489.

de Bruin, J.P., Swinkels, W.A., and De Brabander, J.M. (1997). Response learning of rats in a Morris water maze: involvement of the medial prefrontal cortex. Behav. Brain Res. *85*, 47–55.

Dymecki, S. (1996). Flp recombinase promotes site-specific DNA recombination in embryonic stem cells and transgenic mice. Proc. Natl. Acad. Sci. USA *93*, 6191–6196.

Eichenbaum, H., Dudchenko, P., Wood, E., Shapiro, M., and Tanila, H. (1999). The hippocampus, memory, and place cells: is it spatial memory or a memory space? Neuron *23*, 209–226.

Erickson, J.T., Conover, J.C., Borday, V., Champagnat, J., Barbacid, M., Yancopoulos, G., and Katz, D.M. (1996). Mice lacking brain-derived neurotrophic factor exhibit visceral sensory neuron loss distinct from mice lacking NT4 and display a severe developmental deficit in control of breathing. J. Neurosci. *16*, 5361–5371.

Finkbeiner, S., Tavazoie, S.F., Maloratsky, A., Jacobs, K.M., Harris, K.M., and Greenberg, M.E. (1997). CREB: a major mediator of neuronal neurotrophin responses. Neuron *19*, 1031–1047.

Fritzsch, B., Silos-Santiago, I., Bianchi, L.M., and Farinas, I. (1997). The role of neurotrophic factors in regulating the development of inner ear innervation. Trends Neurosci. *20*, 159–164.

Fryer, R.H., Kaplan, D.R., Feinstein, S.C., Radeke, M.J., Grayson, D.R., and Kromer, L.F. (1996). Developmental and mature expression of full-length and truncated TrkB receptors in the rat forebrain. J. Comp. Neurol. *374*, 21–40.

Gerlai, R., Henderson, J.T., Roder, J.C., and Jia, Z. (1998). Multiple behavioral anomalies in GluR2 mutant mice exhibiting enhanced LTP. Behav. Brain Res. *95*, 37–45.

Gorba, T., and Wahle, P. (1999). Expression of TrkB and TrkC but not BDNF mRNA in neurochemically identified interneurons in rat visual cortex in vivo and in organotypic cultures. Eur. J. Neurosci. *11*, 1179–1190.

Gu, H., Marth, J.D., Orban, P.C., Mossmann, H., and Rajewsky, K. (1994). Deletion of a DNA polymerase beta gene segment in T cells using cell type-specific gene targeting. Science *265*, 103–106.

Henderson, C.E. (1996). Role of neurotrophic factors in neuronal development. Curr. Opin. Neurobiol. *6*, 64–70.

Hogan, B., Beddington, R., Costantini, F., and Lacy, E. (1994). Manipulating the Mouse Embryo: A Laboratory Manual. (Cold Spring Harbor Laboratory Press, New York).

Hostetter, G., and Thomas, G.J. (1967). Evaluation of enhanced thigmotaxis as a condition of impaired maze learning by rats with hippocampal lesions. J. Comp. Physiol. Psychol. *63*, 105–110.

Huang, E., Wilkinson, G., Farinas, I., Backus, C., Zang, K., Wong, S., and Reichardt, L. (1999). Expression of trk receptors in the developing mouse trigeminal ganglion: in vivo evidence for NT-3 activation of TrkA and TrkB in addition to trkC. Development *126*, 2191–2203.

Inagawa, K., Watanabe, S., Tsukada, Y., and Mikoshiba, K. (1988). The role of myelination in learning performance observed in two strains of myelin-deficient mutant mice (shiverer and mld). Behav. Neural Biol. *50*, 184–192.

Inoue, A., and Sanes, J.R. (1997). Lamina-specific connectivity in the brain: regulation by N-cadherin, neurotrophins, and glycoconjugates. Science *276*, 1428–1431.

Iwasaki, Y., Gay, B., Wada, K., and Koizumi, S. (1998). Association of the Src family tyrosine kinase Fyn with TrkB. J. Neurochem. *71*, 106–111.

Jarrard, L.E. (1976). Anatomical and behavioral analysis of hippocampal cell fields in rats. J. Comp. Psychol. *90*, 1035–1050.

Kaplan, D.R., and Miller, F.D. (1997). Signal transduction by the neurotrophin receptors. Curr. Opin. Cell Biol. *9*, 213–221.

Katz, L.C., and Shatz, C.J. (1996). Synaptic activity and the construction of cortical circuits. Science *274*, 1133–1138.

Kellendonk, C., Tronche, F., Casanova, E., Anlag, K., Opherk, C., and Schütz, G. (1999). Inducible site-specific recombination in the brain. J. Mol. Biol. *285*, 175–182.

Kirkby, D.L., and Higgins, G.A. (1998). Characterization of perforant path lesions in rodent models of memory and attention. Eur. J. Neurosci. *10*, 823–838.

Klein, R., Smeyne, R.J., Wurst, W., Long, L.K., Auerbach, B.A., Joyner, A.L., and Barbacid, M. (1993). Targeted disruption of the trkB neurotrophin receptor gene results in nervous system lesions and neonatal death. Cell *75*, 113–122.

Korte, M., Carroll, P., Wolf, E., Brem, G., Thoenen, H., and Bonhoeffer, T. (1995). Hippocampal long-term potentiation is impaired in mice lacking brain-derived neurotrophic factor. Proc. Natl. Acad. Sci. USA *92*, 8856–8860.

Korte, M., Griesbeck, O., Gravel, C., Carroll, P., Staiger, V., Thoenen, H., and Bonhoeffer, T. (1996). Virus-mediated gene transfer into hippocampal CA1 region restores long-term potentiation in brain-derived neurotrophic factor mutant mice. Proc. Natl. Acad. Sci. USA *93*, 12547–12552.

Lessmann, V., Gottmann, K., and Heumann, R. (1994). BDNF and NT-4/5 enhance glutamatergic synaptic transmission in cultured hippocampal neurones. Neuroreport *6*, 21–25.

Levine, E., Dreyfus, C., Black, I., and Plummer, M. (1998). Brain-derived neurotrophic factor rapidly enhances synaptic transmission in hippocampal neurons via postsynaptic tyrosine kinase receptors. Proc. Natl. Acad. Sci. USA *92*, 8074–8077.

Lewin, G.R., and Barde, Y.-A. (1996). Physiology of the neurotrophins. Annu. Rev. Neurosci. *19*, 289–317.

Li, Y.X., Zhang, Y.O., Lester, H.A., Schuman, E.M., and Davidson, N. (1998). Enhancement of neurotransmitter release induced by brain-derived neurotrophic factor in cultured hippocampal neurons. J. Neurosci. *18*, 10231–10240.

Linnarsson, S., Björklund, A., and Ernfors, P. (1997). Learning deficit in BDNF mutant mice. Eur. J. Neurosci. *9*, 2581–2587.

Lipp, H.-P., and Wolfer, D.P. (1998). Genetically modified mice and cognition. Curr. Opin. Neurobiol. *8*, 272–280.

Lipska, B.K., Jaskiw, G.E., and Weinberger, D.R. (1994). The effects of combined prefrontal cortical and hippocampal damage on dopamine-related behaviors in rats. Pharmacol. Biochem. Behav. *48*, 1053–1057.

Lisman, J.E. (1999). Relating hippocampal circuitry to function: recall of memory sequences by reciprocal dentate-CA3 interactions. Neuron *22*, 233–242.

Logue, S.F., Paylor, R., and Wehner, J.M. (1997). Hippocampal lesions cause learning deficits in inbred mice in the morris water maze and conditioned-fear task. Behav. Neurosci. *111*, 104–113.

Mair, R.G., Burk, J.A., and Porter, M.C. (1998). Lesions of the frontal cortex, hippocampus, and intralaminar thalamic nuclei have distinct effects on remembering in rats. Behav. Neurosci. *112*, 772–792.

Martinez, A., Alcantara, S., Borrell, V., Del Rio, J.A., Blasi, J., Otal, R., Campos, N., Boronat, A., Barbacid, M., Silos-Santiago, I., et al. (1998). TrkB and TrkC signaling are required for maturation and synaptogenesis of hippocampal connections. J. Neurosci. *18*, 7336–7350.

Mayford, M., Bach, M.E., Huang, Y.Y., Wang, L., Hawkins, R.D., and Kandel, E.R. (1996). Control of memory formation through regulated expression of a CamKII transgene. Science *274*, 1678–1683.

McAllister, A.K., Katz, L.C., and Lo, D.C. (1999). Neurotrophins and synaptic plasticity. Annu. Rev. Neurosci. *22*, 295–318.

Migaud, M., Charlesworth, P., Dempster, M., Webster, L., Watabe, A., Makhinson, M., He, Y., Ramsay, M., Morris, R., Morrison, J., et al. (1998). Enhanced long-term potentiation and impaired learning in mice with mutant postsynaptic density-95 protein. Nature *396*, 433–439.

Milner, B., Squire, L.R., and Kandel, E.R. (1998). Cognitive neuroscience and the study of memory. Neuron *20*, 445–468.

Minichiello, L., and Klein, R. (1996). TrkB and TrkC neurotrophin receptors cooperate in promoting survival of hippocampal and cerebellar granule neurons. Genes Dev. *10*, 2849–2858.

Minichiello, L., Casagranda, F., Soler Tatche, R., Stucky, C.L., Postigo, A., Lewin, G.R., Davies, A.M., and Klein, R. (1998). Point mutation in trkB causes loss of NT4-dependent neurons without major effects on diverse BDNF responses. Neuron *21*, 335–345.

Misslin, R., Haberkorn, E., and Ropartz, P. (1981). Responses to novelty and changes in behavior across a 3-week postoperative period in hippocampal-lesioned mice. Physiol. Behav. *27*, 413–418.

Montkowski, A., and Holsboer, F. (1997). Intact spatial learning and memory in transgenic mice with reduced BDNF. Neuroreport *8*, 779–782.

Morris, R.G.M. (1982). Place navigation impaired in rats with hippocampal lesions. Nature *297*, 681–683.

Müller, U., Cristina, N., Li, Z.-W., Wolfer, D.P., Lipp, H.-P., Rülicke, T., Brandner, S., Aguzzi, A., and Weissmann, C. (1994). Behavioral and anatomical deficits in mice homozygous for a modified β-amyloid precursor protein gene. Cell *79*, 755–765.

Nagahara, A.H., Otto, T., and Gallagher, M. (1995). Entorhinal-perirhinal lesions impair performance of rats on two versions of place learning in the Morris water maze. Behav. Neurosci. *109*, 3–9.

Nosten-Bertrand, M., Errington, M.L., Murphy, K.P., Tokugawa, Y., Barboni, E., Kozlova, E., Michalovich, D., Morris, R.G.M., Silver, J., Stewart, C.L., et al. (1996). Normal spatial learning despite regional inhibition of LTP in mice lacking Thy-1. Nature *379*, 826–829.

Okabe, S., Collin, C., Auerbach, J., Meiri, N., Bengzon, J., Kennedy, M., Segal, M., and McKay, R. (1998). Hippocampal synaptic plasticity in mice overexpressing an embryonic subunit of the NMDA receptor. J. Neurosci. *18*, 4177–4188.

O'Keefe, J., and Nadel, L. (1978). The hippocampus as a cognitive map. (London: Oxford University Press).

Olton, D.S., Walker, J.A., and Gage, F.H. (1978). Hippocampal connections and spatial discrimination. Brain Res. *139*, 295–308.

Packard, M.G., and Teather, L.A. (1998). Amygdala modulation of multiple memory systems: hippocampus and caudate-putamen. Neurobiol. Learn. Mem. *69*, 163–203.

Patterson, S.L., Abel, T., Deuel, T.A., Martin, K.C., Rose, J.C., and Kandel, E.R. (1996). Recombinant BDNF rescues deficits in basal synaptic transmission and hippocampal LTP in BDNF knockout mice. Neuron *16*, 1137–1145.

Penn, A.A., Riquelme, P.A., Feller, M.B., and Shatz, C.J. (1999). Competition in retinogeniculate patterning driven by spontaneous activity. Science *279*, 2108–2112.

Phillips, R.G., and Ledoux, J.E. (1992). Differential contribution of amygdala and hippocampus to cued and contextual fear conditioning. Behav. Neurosci. *106*, 274–285.

Pozzo-Miller, L.D., Gottschalk, W., Zhang, L., McDermott, K., Du, J., Gopalakrishnan, R., Oho, C., Sheng, Z.H., and Lu, B. (1999). Impairments in high-frequency transmission, synaptic vesicle docking, and synaptic protein distribution in the hippocampus of BDNF knockout mice. J. Neurosci. *19*, 4972–4983.

Rossi-Arnaud, C., and Ammassari-Teule, M. (1998). What do comparative studies of inbred mice add to current investigations on the neural basis of spatial behaviors? Exp. Brain Res. *123*, 36–44.

Shieh, P.B., and Ghosh, A. (1997). Neurotrophins: new roles for a seasoned cast. Curr. Biol. *7*, R627-R630.

Tsien, J.Z., Chen, D.F., Gerber, D., Tom, C., Mercer, E.H., Anderson, D.J., Mayford, M., Kandel, E.R., and Tonegawa, S. (1996). Subregion- and cell type-restricted gene knockout in mouse brain. Cell *87*, 1317–1326.

Xu, M., Moratalla, R., Gold, L.H., Hiroi, N., Koob, G.F., Graybiel, A.M., and Tonegawa, S. (1994). Dopamine D1 receptor mutant mice are deficient in striatal expression of dynorphin and in dopamine-mediated behavioral responses. Cell *79*, 729–742.

Yu, X.M., Askalan, R., Keil, G.J., and Salter, M.W. (1997). NMDA channel regulation by channel-associated protein tyrosine kinase Src. Science *275*, 674–678.